



2001

The effect of ionizing radiation on human brain

David Spence

Follow this and additional works at: https://trace.tennessee.edu/utk_interstp2

Recommended Citation

Spence, David, "The effect of ionizing radiation on human brain" (2001). *Senior Thesis Projects, 1993-2002*.

https://trace.tennessee.edu/utk_interstp2/75

This Project is brought to you for free and open access by the College Scholars at TRACE: Tennessee Research and Creative Exchange. It has been accepted for inclusion in Senior Thesis Projects, 1993-2002 by an authorized administrator of TRACE: Tennessee Research and Creative Exchange. For more information, please contact trace@utk.edu.

The effect of ionizing radiation on human brain

By
David Spence

College Scholars Project
April 27, 2001

ABSTRACT

Objective: To test the hypothesis that fractionated radiation therapy of less 50 Gy is associated with a dose-related change in the T1 of normal brain tissue, and that these changes are detectable by quantitative MRI.

Methods: A total of 33 patients, who were being treating for a primary brain tumor, received qMRI examinations prior to conformal radiation therapy and at 3 weeks, 5 weeks, and 3-month intervals following treatment. A T1 map was generated for each patient, and radiation dose maps were superimposed over the corresponding T1 maps. Changes in white matter and gray matter T1 were then evaluated longitudinally as a function of radiation dose and time since treatment. Patient age, tumor site, and clinical variables were also including in the analysis.

Results: There was a dose-dependent decrease in T1 over time in the white matter that received greater than 20 Gy that became significant after 6 months. There was no significant change over time in T1 of gray matter that received less than 50 Gy. However, gray matter close to the tumor was inherently different.

Conclusion: The results we obtained were the first dose-response data taken from the pediatric brain *in vivo*. Our findings conclude that white matter is far more sensitive to radiation than gray matter even at lower doses. White matter is resistant to a radiation dose of less than 20 Gy, while gray matter is only resistant at greater than 50 Gy. Also, the tumor does seem to have an effect on the tissue that immediate surrounds it, with the effect being larger in patients with a infratentorial tumor. In addition, conformal radiation may substantially benefit the patients by minimizing the radiation dose and ultimately the damage that the brain tissue receives during therapy.

INTRODUCTION:

Radiation has been used in the treatment of cancer since the early 1900's. In 1895, Wilhelm Roentgen discovered what would later be called x-rays, and as early as 1902, x-rays were being used to treat cancer, giving birth to the field of radiotherapy. Before long, doctors and scientists were using x-rays to treat almost every kind of disease. It did not take long, however, for people to realize that harmful side effects can be involved with using x-rays to treat disease. In fact, many of the early scientists and physicians who worked with x-rays developed fatal conditions brought about by extensive exposure to radiation. In the 1930's, there was an increased interest in the effects of radiation on all tissues, and out of that interest grew the field of radiobiology, (1). Over the next thirty years, the fields of radiotherapy and radiobiology grew together as advancements of radiation therapy were coupled with a growing awareness of the effects of radiation on tissues. Currently, radiation oncology, which is the field centered around the use of ionizing radiation in the treatment of cancer, is one of the fastest growing medical fields. In 1996, approximately 60 percent of cancer patients received some type of radiation therapy (2). Unfortunately, the growth of radiation oncology has been aided by the growth in the incidence of cancer, as well as by advancements in the understanding and delivery of ionizing radiation.

One of the central questions of radiation oncology that has fueled a great deal of research is the how well does normal tissue tolerate ionizing radiation. As techniques for delivering radiation to the desired target continue to improve, the rate of prolonged remission and even achievement of a "cure" continues to increase dramatically; however,

with an increasingly large group of survivors comes a growing concern for toxicities and long-term effects of ionizing radiation. By definition, ionizing radiations are those which are capable of interacting with atoms and molecules in the body to produce biological effects (3). As the beams of radiation pass into the body, they are absorbed and released locally, and thus the energy of the beam when it reaches the target tissue is dependent on the depth of the tissue from the skin and the density of tissues the beam penetrates (3). Thus, it is apparent that the tissues surrounding the target tissue also receive a considerable amount of radiation, and traditionally, the surrounding tissue receives more than the target. As a result, it is imperative that the amount of radiation received by this tissue is not only monitored, but also kept to a minimum.

An area where understanding toxicities and long-term effects is particularly important is the brain. According to Shrieve et al., radiation therapy is the single most active treatment for glial tumors, which are the most common type of brain tumor, and radiation doses up to 60 Gy yield dose-related increases in patient survival (4). Yet, DeAngelis et al. have shown that even relatively low doses of radiation to the brain causes up to a 3- to 7-fold increase in the incidence of glial tumors (5). Thus, there is a dichotomy set up between the benefits and ill-effects of irradiation in the treatment of brain tumors.

The potential for radiation-induced injury to the CNS and, in particular, the brain limits the amount of radiation that can be safely delivered in the treatment of a brain tumor (6). As a result, new techniques have been developed to limit the amount of radiation that the normal tissue surrounding the tumor receives. One such technique is three-dimensional (3D) conformal radiation therapy. The basis of conformal radiation

therapy is to deliver the desired amount of ionizing radiation to the target tissues, so that the target receives a uniform dose and the dose to the surrounding tissue is kept below a level that might produce adverse side effects (7). In order to accomplish this feat, the ionizing radiation is delivered from multiple angles in three dimensions, as the name suggests. Thus, the only tissue that receives the full dosage is the tissue that lies within the margin of the target.

While 3D conformal radiation therapy does successfully limit the amount of brain tissue that is exposed to the full dosage, a larger portion of the brain is exposed to a lower dose of radiation. This fact begs the question of what are the effects of low-dose radiation on normal brain tissue. Several studies have shown that radiation doses of less than 50 Gy can cause serious long-term effects such as loss of neurocognitive functioning or marked behavioral effects (8-17). While these studies suggest that radiation can be damaging at relatively low doses, there is a need for an effective means of evaluating radiation effects at lower doses.

Magnetic resonance imaging (MRI) is known to be able to detect white matter changes in as many as 50% of patients who have received radiation treatment for a brain tumor (18-21). Yet, other studies have shown that white matter changes that are detectable by conventional MRI (cMRI) are not well correlated with the severity of neurological outcomes (22). Thus, there is a need for a more sensitive and a quantitative means of evaluating the effect of radiation on brain tissue.

Earlier studies in our laboratory suggest that quantitative MRI (qMRI) may be more sensitive to changes in brain tissue than cMRI, particularly in those changes that follow radiation treatment (23). In a preliminary study, we found that ionizing radiation

is associated with qMRI abnormalities in white matter but not gray matter. In the white matter, we found that there was a significant dose-dependent decrease in the spin-lattice relaxation time (T1) six months following the initiation of radiation therapy, and this decrease existed in tissue that received less than 40 Gy. However, in our preliminary study, we only evaluated a small sample of patients, which limited our study. Therefore, in this study, we expand the sample of patients in order to determine if our preliminary assumption that there is dose-dependent response to radiation of less than 40 Gy in the white matter of patients who are undergoing radiation therapy is correct. Moreover, we wish to investigate a transient decrease in T1 that occurred in the third week of follow-up in our preliminary data. Our hope is to find a standard acute response that will allow us to assess the progress of patients who are undergoing radiation therapy, and finally, to determine if conformal radiation therapy does offer a benefit to patients by lowering the amount of healthy brain tissue that receives high amounts of radiation.

METHODS

Protocol overview

In July of 1997, patient enrollment was opened for a new protocol at St. Jude Children's Research Hospital entitled "A Phase II study of image-guided radiation therapy for pediatric CNS tumors and quantification of radiation-related CNS events".

The eligibility criteria for the protocol included the following:

- Patient age at diagnosis: 1.5-21 years
- Histologically-confirmed primary brain tumor

- Unifocal tumor (no dissemination of tumor within or beyond the central nervous system)
- Histologic type requiring only focal irradiation
- No prior radiation therapy
- No ongoing chemotherapy (excluding corticosteroids)
- Adequate performance status (ECOG 0-3)

Following a detailed description of the protocol, the parents or guardians of all the children signed an informed consent. Patients then received an MRI exam which included both cMRI and qMRI prior to the initiation of the radiation therapy. During the qMRI portion of the examination, images were acquired that enabled us to measure white matter T1 and gray matter T1. The same examination was repeated at weeks 3 and 5 of the radiation therapy, and every 3 months after the initiation of the radiation therapy. The pre-treatment examination allowed each patient to act as their own control, and thus we were able to detect small changes in T1 that may be attributed to radiation therapy.

Description of patients

A total of 33 patients who were enrolled on the above protocol were used in this study. All of patients have completed their radiation therapy. Patient age ranged from 2.3 to 18.7 years with the mean age of 9.1 years. Each of the patients was treated with conformal radiation therapy directed at the primary site of disease with a total dose prescription of either 54.0 or 59.4 Gy. Most of the patients (n=18) received a minimum of 5 qMRI examinations, and additional examinations were obtained at week 39 (n=15) and week 52 (n=11) for some of the patients.

Conventional MRI

All MR imaging was performed on a 1.5 Tesla MR imager (Siemens Medical Systems, Iselin, NJ), using a standard Siemens quadrature head coils. Conventional T1-weighted gradient echo MR image sets were acquired across the brain in sagittal and transverse planes. These images were used to select a slice level for the qMRI examinations. In addition, T2- and proton-density weighted turbo spin-echo images were acquired to screen patients for progressive disease. In patients with progressive disease, we would be unable to determine if any acute changes in T1 were due to radiation or the effect of the tumor, and therefore they were excluded from the study. The total amount of time it took to acquire these images was approximately 11 minutes.

Quantitative MRI

Quantitative MR imaging of T1 was done with a precise and accurate inversion-recovery (PAIR) method and its improved version (TurboPAIR). Each method was developed, optimized, and validated in the diagnostic imaging lab at St. Jude Children's Research Hospital (24-29). The time required for imaging for the TurboPAIR sequence is 4 minutes versus the 14 minutes that is required by the PAIR sequence. A single transverse slice at the level of the basal ganglia was selected for each of the patients, so that the same structures were viewed for all of the patients.

Measurement of T1

After we had acquired the qMRI images, we then transferred the images to a Silicon Graphics Indy workstation for further analysis. The pixels that were identified as noise were excluded by a statistical criteria that was established by Gene Reddick (30), and the remaining pixels were submitted to a curve-fitting procedure (24,30, 31). The T1 equation was solved for α (spin-density factor corrected for T2 losses), k (cosine of the effective flip angle of the inversion pulse), and T1 in each pixel. The T1 value was used to generate a parametric T1 map of the image, wherein the pixel grayscale value is equivalent to the relaxation time in msec.

Segmentation of qMRI images

The qMRI images were then analyzed using a fully automated neural network algorithm (32, 33), that was adapted to specifically segment the tissues in TurboPAIR images (34). This method can segment tissue into 9 separate ranges of T1 values, each of which correlate directly with a type a category of tissue. These categories are gray matter (GM), white matter (WM), cerebrospinal fluid (CSF), partial volume of GM and WM, partial volume of GM and CSF, or background. The non-normalized signal intensity from each pixel in the 4 TurboPAIR base images was used as input to a 3 x 3 single-layer Kohonen self-organizing map (SOM). After image segmentation was completed, each of the 9 levels in the segmented image was manually classified as one of the six categories above, and a pseudo-color image of the brain was created (33).

The pseudo-color images were then imported into Adobe Photoshop 4.0.1, and extrameningial tissues were erased manually using the standard Photoshop tools. In the segmented image, the yellow pixels correspond to GM, and the green pixels correspond

to WM. All of the other colors, include the lime green pixels, which correspond to partial volume of GM and WM, were not analyzed any further. The central GM and WM was also erased from the image because we lack adequate control data from which to determine expected T1 values for GM and WM tracts in the central structures of the brain (25). In addition, in many of the patients, the dosimetric lines were placed too close to each other to accurately assess T1 of the tissue as a function of RT dose.

Conformal radiation therapy

Conformal 3-D treatment plans employing 4-25 beams were developed using the “PLan University of North Carolina” treatment planning system. The majority of treatments were delivered on MLC-equipped Siemens Primus and Primart linear accelerators. Patients were immobilized with a stereotactic head frame, a thermoplastic face mask, or a vacuum bag molded to the patient. General anesthesia was used when necessary. Treatment-planning guidelines specified a 10mm anatomically defined clinical target volume (CTV) for ependymoma, low-grade astrocytoma or low-grade neuronal tumors, and craniopharyngioma. Patients with high-grade astrocytoma or high-grade neuronal tumors were treated with a 20mm anatomically defined CTV. The geometric margin used to define the planning target volume was fixed at 5mm for all patients independent of immobilization. Targeting followed ICRU guidelines (35) and tissue outside the target volume is regarded as normal, for the purposes of this analysis. Isodose contours were generated for each of the patients in a plane that corresponded to the slice level of the qMRI image. The contours included dose levels that ranged from 5 Gy to 54.9 Gy and were in 5 Gy increments. Due to the fact that not all of the patients

had tumor in the level of the slice, some of the patients did not have T1 maps that included the highest dose of radiation therapy.

Analyzing T1 as a function of radiation

In order to determine the relationship between T1 and the radiation dose, the isodose contours for each patient were superimposed onto the corresponding segmented T1 maps. Tissue T1 was then calculated as a function of radiation dose for both white and gray matter, and the T1 was recorded as a function of time since radiation therapy was delivered. This information was then compiled into a data set which included: tissue type (GM and WM); radiation dose, classified into one of 8 categories (<5 Gy, 5 to <10 Gy, 10 to <20 Gy, 20 to <30 Gy, 30 to <40 Gy, 40 to <50 Gy, 50 to <54 Gy, and ≥ 54 Gy); and time since the radiation treatment in 3 week, 5 week, and 3 month intervals.

Statistical tests

In our study, we wanted to examine the longitudinal trends of T1 in the WM and GM of the patients as a function of the radiation dose. Because each patient received multiple qMRI examinations, the tissue T1 times were inter-correlated. As a result, we used the mixed linear model (36, 37) to analyze the data, in which T1 is the response variable, each patient is treated as a cluster, the day from initiation of radiation therapy is the longitudinal variable, and the radiation dose to tissue is the primary covariate variable. The age of the patient at the initiation of treatment was also included in the model, because age is known to have an effect on T1 (26). Initially, we used a longitudinal model, freeing the linear longitudinal trend in T1 in each brain tissue from

the influence of radiation dosage. We were able to use this model by assigning radiation dose as a categorical variable, rather than as an ordinal variable. This model strongly suggested that the estimated intercepts and slopes of the longitudinal trends in T1 changed in accordance with the magnitude of radiation dose. Because of this finding, we then fitted our data into a surface model, in which the intercepts and slopes of the longitudinal trends in T1 were linearly related to the radiation dosage to the brain tissue. The T1 trends predicted by the surface model matched well to those in the simple longitudinal model; however, we believe that the surface model gave a better estimation of the T1 trends by eliminating a layer of variability due to error (23).

In addition, we wanted to determine if T1 of either WM or GM changed acutely during the first 5 weeks of radiation therapy. In order to accomplish this, we generated scatterplots of T1 at each radiation dose level over time, with each patient plotted separately. Visual inspection of these scatterplots was used to determine if there were trends in T1. We also wanted to determine whether trends in WM T1 were influenced by clinical variables such as tumor site (infratentorial *vs* supratentorial) or the use of chemotherapy and steroids (yes *vs* no). We examined longitudinal trends in T1 as a function of the major independent variables (radiation dose, patient age, and time since starting treatment).

RESULTS

Patient data

As discussed in the protocol, all of the patients' diagnoses were biopsy-proven and included tumors of the following types: ependymoma (13 patients), juvenile pilocytic astrocytoma (9 patients), craniopharyngioma (5 patients), low-grade astrocytoma (1 patient), anaplastic astrocytoma (1 patient), ganglioglioma (1 patient), astroblastoma (1 patient), pleomorphic xanthoastrocytoma (1 patient), and glioblastoma multiforme (1 patient). The mean tumor size at the time of treatment was 3.7 cm, with a range of 2.0 cm to 6.5 cm.

Conventional MRI examinations

As discussed, conventional MRI (cMRI) films were used to identify patients with progressive disease. Only one patient was censored because disease progression was noted about 6 months after the radiation therapy. However, a second patient was censored because their last MRI examination was completed nearly 2 months after the scheduled time interval, and thus the qMRI data for that patient would be invalid. All of the other scheduled examinations were completed at close to the scheduled times (23). This allowed us to pool the patient examinations by time since radiation treatment.

Brain T1 as a function of radiation dose

Brain T1 was measured in a total of 1,692 separate regions of interest (ROIs) among the 159 examinations evaluated (Table 1). A roughly equal number of ROIs were evaluated in white matter and gray matter, so the sensitivity of the method should be comparable for radiation-related changes in both types of tissues. Roughly 70% of the data analyzed were acquired within 3 months of initiation of radiation treatment, and only

8% of the data were acquired after 1 year. Therefore, our analysis will be better suited to analyzing T1 changes in the early follow-up intervals, and aid us in evaluating acute changes in the tissue.

White matter T1 at each of the separate dose levels is plotted (Figure 2). This plot suggests that white matter exposed to greater than 20 Gy shows a reduction in T1 by week 40 that persisted at week 53. As seen in the figure, there may be a substantial increase in T1 at the highest dose level of radiation at week 12, but this increase was not statistically significant and may be due to a breakdown in the blood brain barrier. Individual dose-response curves for white matter T1 at each time interval are also plotted (Figure 3). This plot illustrates a downward trend in the T1 dose-response curves at follow-up intervals of 6 months or longer. There is also a suggestion that T1 is elevated near the tumor by the end of treatment (week 13), and that white matter T1 immediately adjacent to the tumor tends to be high.

Gray matter T1 at each of the separate dose levels is also plotted (Figure 4). This plot suggests that gray matter exposed to greater than 50 Gy has a lower T1 at all time points than gray matter exposed to less than 50 Gy. Individual dose-response curves for gray matter T1 at each time interval are also plotted (Figure 5). There again appears to be a downward trend in the T1 dose-response curves except for week 26, when T1 is generally elevated except immediately adjacent to the tumor.

A comparison of observed and expected values of T1 for white matter and gray matter is shown in Table 2. Observed T1 for white matter and gray matter was calculated from all patients evaluated pre-treatment and at the 39 week examination, and the tabulated values are for brain tissue exposed to less than 5 Gy. Expected values were

determined by modeling T1 data from 173 healthy people. Prior to radiation treatment, observed white matter T1 was higher than expected ($p < 0.0002$), whereas observed gray matter T1 was significantly lower than expected ($p < 0.0001$). By the end of 39 weeks of follow-up, observed white matter T1 became more normal, although it was still significantly higher than expected ($p < 0.003$). Gray matter T1, however, was still significantly and substantially less than expected ($p < 0.0001$).

Brain T1 is known to decrease with age in healthy subjects in both white and gray matter (25, 26). The average follow-up period lasted 0.8 years, between the average ages of 9.1 to 9.9 years. During this time interval, T1 is expected to change by -0.6% in white matter and -0.9% in gray matter, as a function of age alone. The actual change that occurred in the study was -2.9% in white matter and -2.1% in gray matter. These changes are roughly 5 times larger than expected for white matter and 2 times larger for gray matter, indicating that age is probably not the significant confounder in this dataset.

Changes in white matter T1 were also analyzed as a function of radiation dose after adjusting for the age of the patients (Table 3). In every case, the slope of the dose-response relationship was negative, suggesting that white matter T1 declines after radiation treatment. However, white matter exposed to less than 20 Gy had no significant radiation-related change in T1, while white matter that was exposed to 20 Gy or greater did show a significant decrease in T1. While the decrease was still relatively low for the white matter that received 20 to 30 Gy, our results show that radiation of greater than 20 Gy does have a significant change in T1 that is consistent with the trend seen in Figure 2.

Changes in gray matter T1 were also analyzed as a function of radiation dose after adjusting for the age of the patients (Table 4). This analysis revealed no significant

radiation-related changes in gray matter T1 at any dose level less than 59 Gy. These results suggest that gray matter is resistant to radiation of less than 59 Gy. However, we noted earlier that in our plot of gray matter T1 over that gray matter T1 was low prior to treatment and remained low throughout the duration of the follow-up period.

Both white matter and gray matter exposed to higher doses of radiation are different from white and gray matter exposed to lower doses of radiation (Table 5). In white matter, this trend does not become significant until 6 months into the follow-up. However, for gray matter there is a significant dose-response relationship even at the time interval before the radiation treatment began. Since gray matter closest to the tumor receives the highest dose of radiation, this finding indicates that the gray matter closest to the tumor is inherently different from the gray matter that is distant from the tumor.

Effect of clinical variables on white matter T1

A mixed-model analysis was used to determine whether clinical variables had an impact on measured T1 in white and gray matter. In the model, the use of chemotherapy and steroids were confounded into one factor, because the use of chemotherapy prior to radiation treatment was highly correlated with the use of steroids during treatment according to a chi-square test. In our analysis, we found that the effects of chemotherapy and steroids were not significant in the longitudinal trend of T1 in either white or gray matter.

We also investigated the impact of the tumor site on T1 prior to the radiation treatment (Table 6). When we divided the patients into those who had infratentorial tumors (IT) and those with supratentorial tumors (ST), we found that in gray matter, the

relationship between T1 and radiation dose at baseline was only significant in patients with IT tumors, in spite of the fact that when all of the patients were examined together, there was a significant dose-response relationship in gray matter. In white matter, we also found a significant relationship between T1 and radiation dose at baseline in those patients with IT tumors, even though when the patient were evaluated as a whole, there was no such relationship. This finding may suggest that IT tumors differ from ST tumors in how they affect distant brain. However, this finding may also be related to patient age, as the 13 patients with IT tumors had an average age of 5.5 years, and the 20 patients with ST patients had an average age of 11.4 years. Thus, the tumor proximity effect may only be attributed to patient age, with the effect being larger in younger patients.

Interestingly, the tumor type had no significant impact on the decline of T1 in response to radiation. For example, patients with glial tumors were not significantly different from patients with nonglial tumors.

DISCUSSION

In this study, we sought to obtain radiation dose-response data that would allow us to determine if radiation therapy affected brain tissue T1 in children at dose levels lower than what is known to cause damage. In doing so, we collected the first radiation dose-response data to be derived from the pediatric brain *in vivo*. These results showed that in white matter, radiation at a dose of greater than 20 Gy was associated with a decrease in T1 over time, a finding that became significant at 6 months. These results confirm that our method of T1 mapping is not only sensitive to radiation related changes

in the human brain, but also more sensitive to such changes than cMRI, as most cMRI studies show little to no evidence of radiation damage below 54 to 60 Gy (38).

While our method proves to be more sensitive, our findings that changes in brain tissue may occur at radiation doses less than 54 Gy is not new. Many neurologic, neurocognitive, and behavior effects have been observed at radiation doses of less than 50 Gy, especially in children (8-17). Prior studies with cMRI have suggested that the primary effect of radiation therapy on human brain tissue is an increase in the signal intensity of white matter, which is consistent with edema (18-21). Edema is expected to produce an increase in T1 in white matter since water has a long T1 time (21). However, our study showed a decrease in T1 over time in response to radiation therapy. This apparent discrepancy may be partially due to the fact that the segmentation process we used would have classified edematous white matter as partial volume of gray and white matter. Thus, our study analyzed only “pure” white matter, and excluded the edematous white matter that may have masked a decrease in T1 of white matter in earlier studies. In addition, radiologists did not note any extensive edema in any of our patients while reading their films, but since edema visible by cMRI usually occurs at longer time intervals and at higher radiation doses, we feel that our results do not contradict earlier studies (18-21).

Our results also suggest that white matter is more vulnerable to low-dose radiation than gray matter. This conclusion is consistent with earlier histological studies that reported extensive radiation-related damage to white matter but not gray matter (39). More recent histological evidence suggests that acute radiation-induced dementia in patients is associated with diffuse demyelination, astrocytic gliosis, and necrosis in white

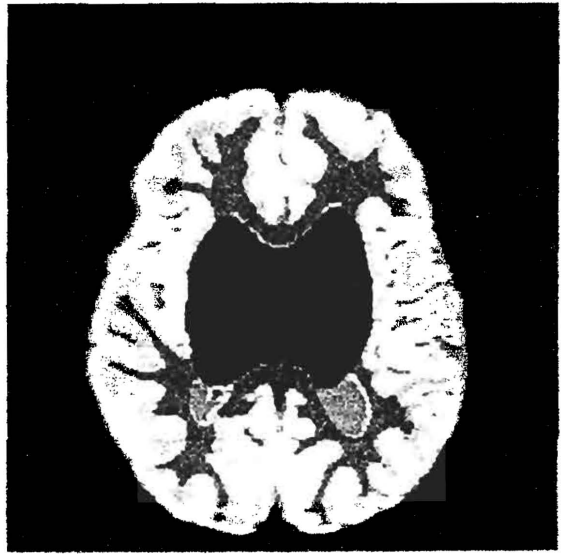
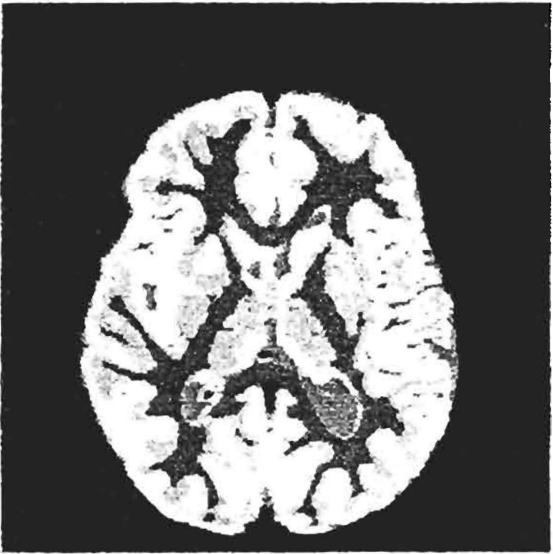
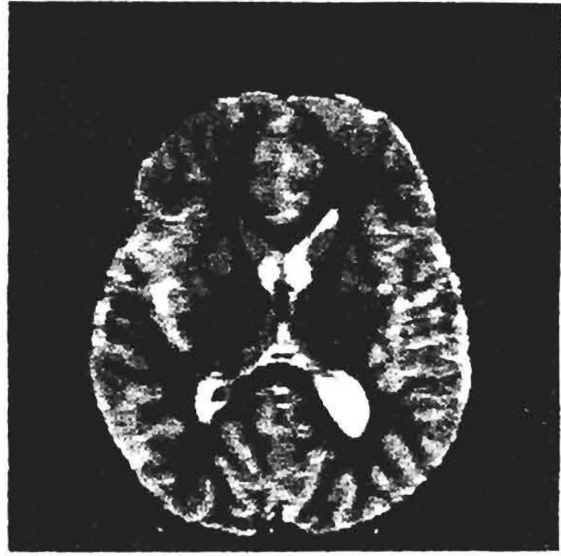
matter, without any apparent damage to gray matter (10). Numerous other studies have demonstrated that white matter is far more sensitive to radiation than gray matter (21, 33, 40, 41); however, the question of why white matter is more sensitive to radiation-related changes in T1 remains unanswered. It has been hypothesized that the primary mechanism for damage is vascular endothelial injury (42). If this is true, however, then it is difficult to see how white matter is more vulnerable than gray matter to radiation, because the regional blood volume of gray matter is approximately twice as high as that of white matter (43), and the metabolic rate of gray matter is also substantially higher than in white matter (44). Both of these factors would suggest that gray matter instead of white matter would be more sensitive to radiation-related damage.

Perhaps our most important finding is that white matter that has been exposed to 20 Gy or greater differs significantly from white matter exposed to less than 20 Gy 6 months into follow-up, suggesting that white matter subjected to relatively low amounts of radiation may still be suffering damage. While the radiation-related decrease is only marginally significant in the tissue that receive 20 to 30 Gy, the significance becomes very obvious in the tissue that receives greater than 30 Gy (Table 5). In spite of the fact that we do not yet understand the pathological basis for the change in T1 in white matter, and reduction in T1 has not been correlated with adverse cognitive outcomes or risk of tumor progression, we can assert that some change is taking place in response to the radiation treatment at much lower doses than has been previously reported.

These findings provide evidence that three-dimensional conformal radiation treatment does indeed offer a substantial benefit to patients, as we suspected. Conformal radiation therapy aims to deliver a uniform dose to the target site while keeping the

amount of brain tissue that receives high amount of radiation to a minimum. In doing so, this technique substantially reduces the amount of healthy brain tissue that receives a level of radiation that may produce harmful side effects, which we have demonstrated to be as low as 20 Gy.

Finally, the finding that the decrease in T1 in white matter does not become significant until nearly six months also helps to answer our hypothesis that there is a transient decrease in T1 3 weeks following the initiation of treatment. Earlier results had suggested that there was a decrease, but this discrepancy can be attributed to a small sample size. As we enlarge the sample size and increase the data set by over 40%, we saw this apparent acute response go away. This discouraged our hopes of finding an acute response to radiation that could be used to evaluate and identify patients who were responding either positively or negatively to their treatment. Such a response would allow physicians to adjust the patients treatment plans according, and thereby prevent any excessive damage to the healthy brain tissue.



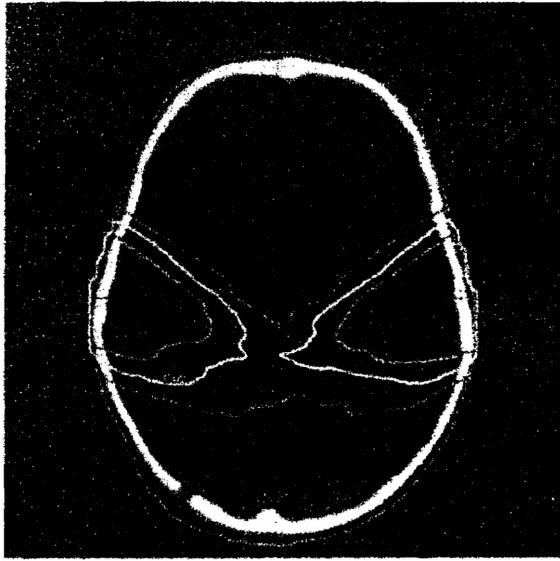


Fig. 1

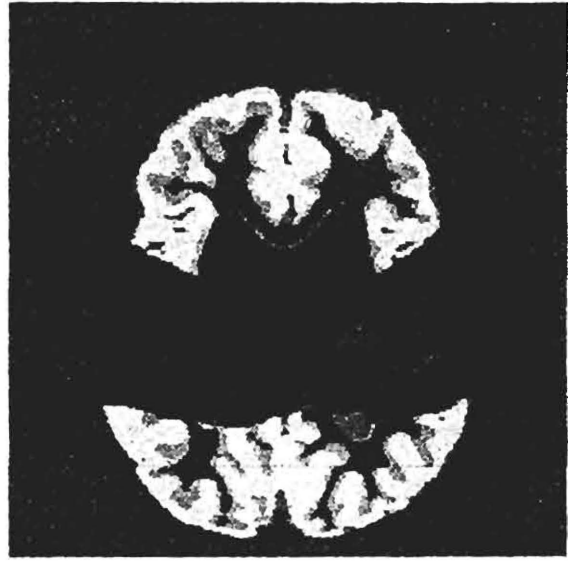


Fig. 2

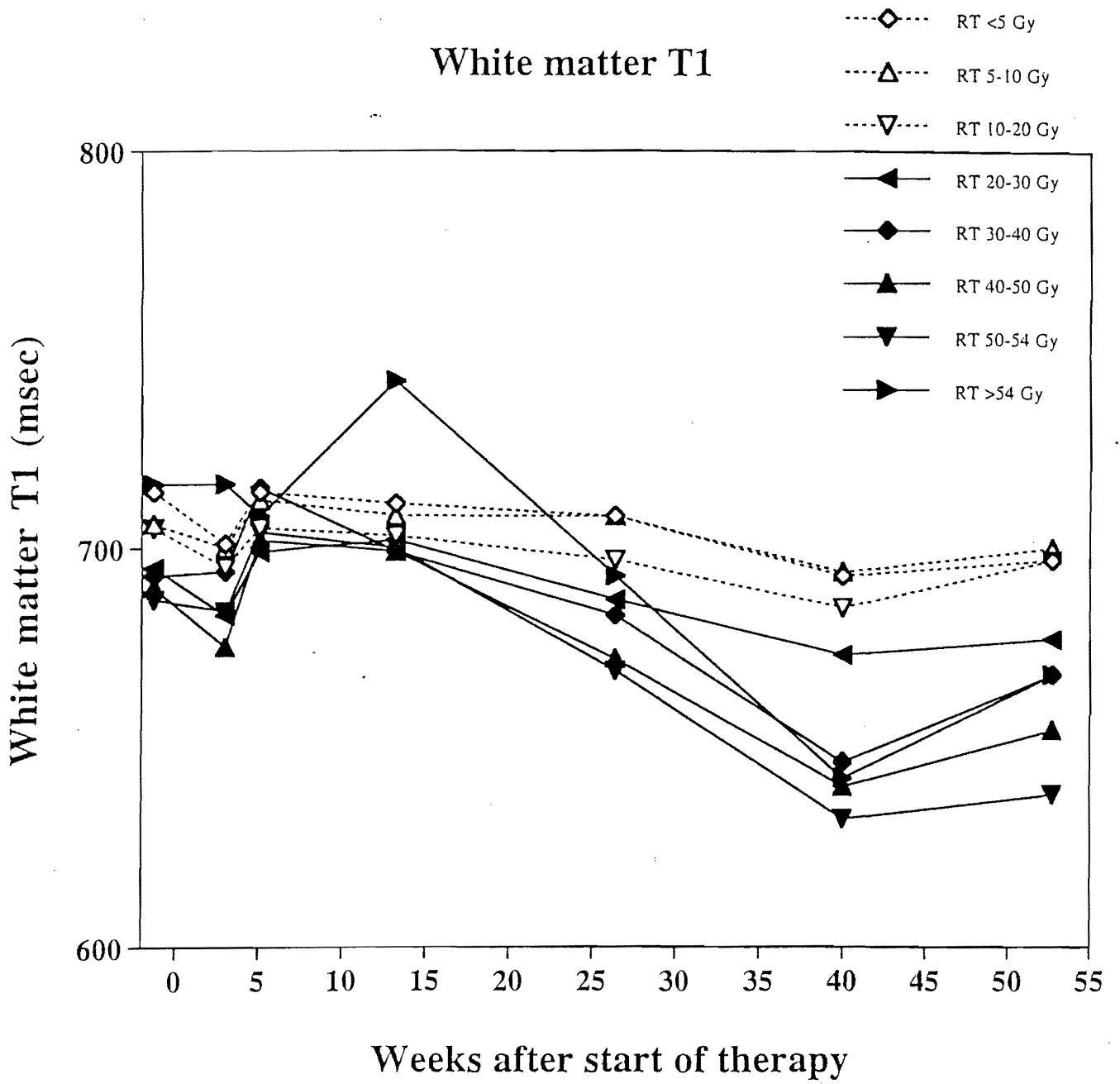


FIGURE 3.

Dose-response curves in WM

- ◇--- WM @ wk 0
- △--- WM @ wk 3
- ▽--- WM @ wk 5
- ◁--- WM @ wk 13
- ◆— WM @ wk 26
- ▲— WM @ wk 40
- ▶— WM @ wk 53

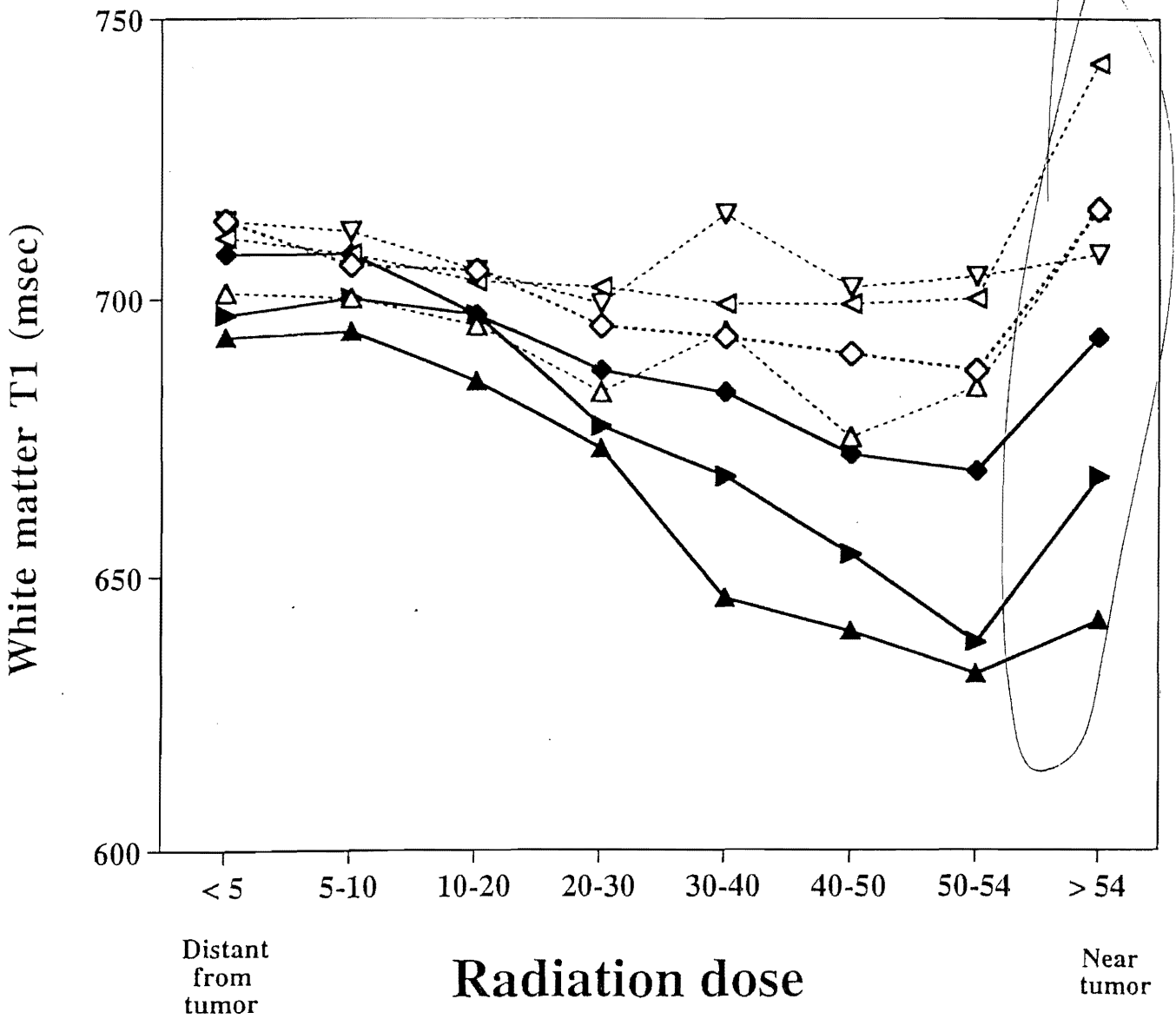


FIGURE 3.

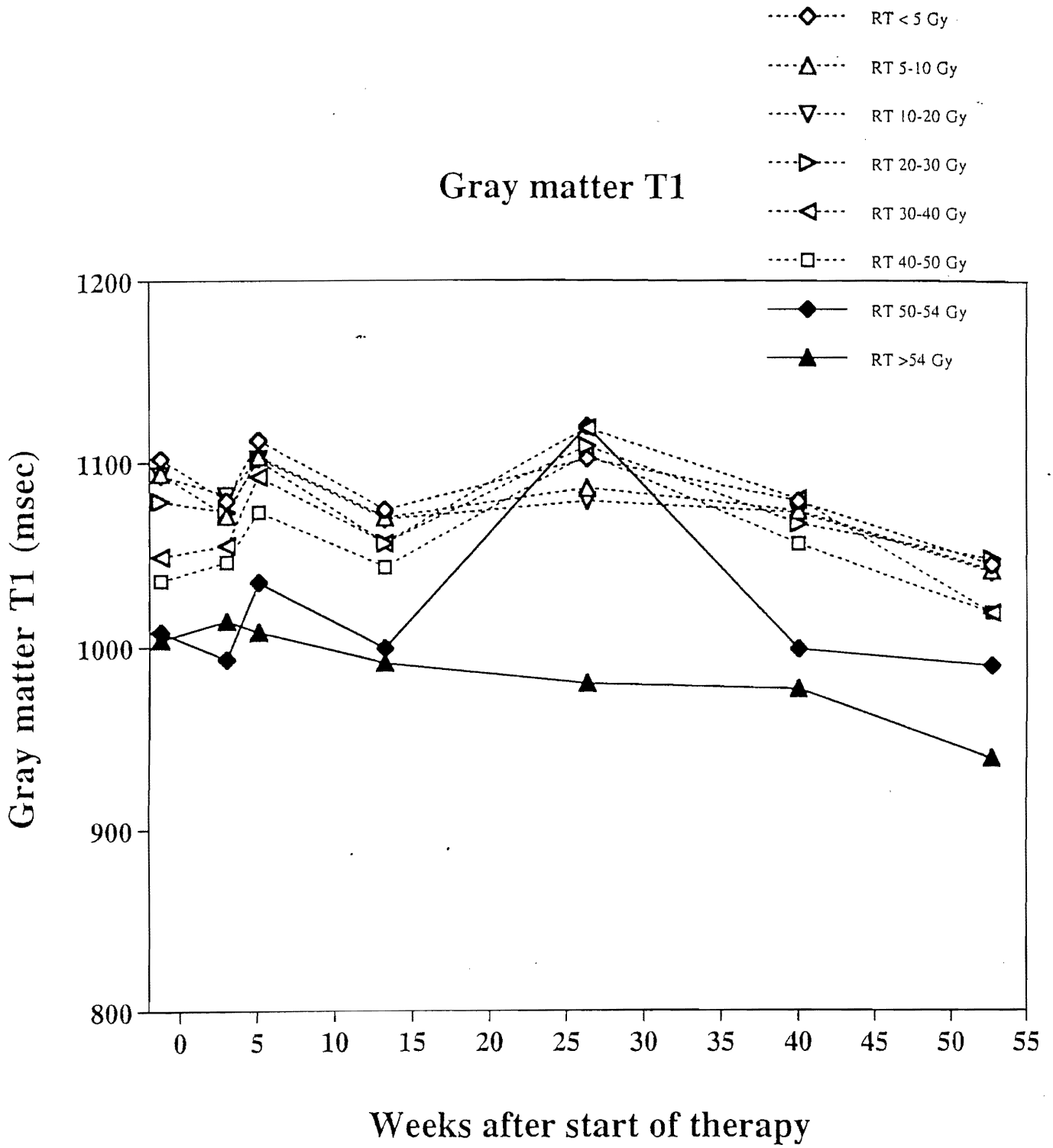


FIGURE 4.

Dose-response curves in GM

- ◇--- GM @ wk 0
- △--- GM @ wk 3
- ▽--- GM @ wk 5
- ◁--- GM @ wk 13
- ◆— GM @ wk 26
- ▲— GM @ wk 40
- ▶— GM @ wk 53

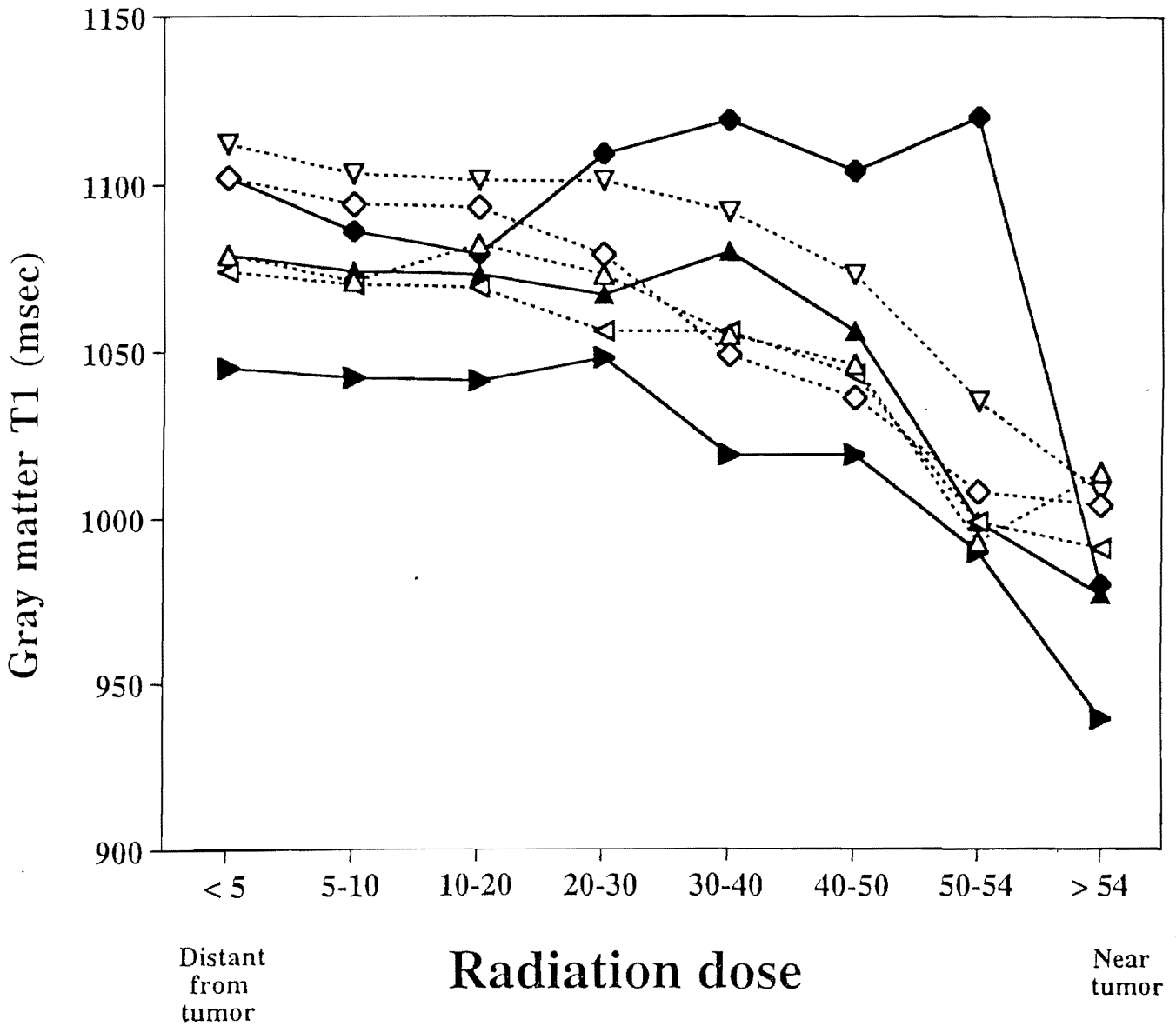


FIGURE 5.

T1 data collected at each time point

Number of ROIs evaluated

Exam	White matter	Gray matter
Pre-RT	174	173
Week 3	141	140
Week 5	130	139
Week 13	147	142
Week 26	101	114
Week 40	82	82
Week 53	62	65
Total ROIs evaluated =	837	855

Table 1. Summary of the number of regions of interest (ROIs) evaluated at each examination in both white matter and gray matter.

Comparison of observed and expected T1 in gray matter and white matter of patients

Tissue	Observed T1 (+SD)	Expected T1 (+SD)	Δ	Two-sided t-test P=
At Start of RT				
WM	714 (\pm 78) n = 33	663 (\pm 24) n = 173	+ 7.7 %	0.0002
GM	1102 (\pm 129) n = 31	1209 (\pm 50) n = 169	- 8.9 %	< 0.0001
At 39 weeks of follow-up				
WM	693 (\pm 43) n = 15	659 (\pm 24) n = 173	+ 5.2 %	0.003
GM	1079 (\pm 76) n = 14	1198 (\pm 50) n=169	- 9.9 %	<0.0001

Table 2. A comparison of observed and expected mean T1 values for white matter (WM) and gray matter (GM) exposed to ≤ 5 Gy. The observed values are the average of the 33 patients evaluated during the pre-treatment and week 39 examination.

White matter T1 as a function of radiation dose

Radiation dose	Intercept (+SD)	Slope (+SD)	p-value
< 5 Gy	713 ± 9	- 0.06 (±0.03)	NS
5 to < 10 Gy	707 ±10	- 0.04 (±0.03)	NS
10 to < 20 Gy	704 ± 9	- 0.04 (±0.03)	NS
20 to < 30 Gy	698 ± 9	- 0.08 (±0.03)	0.05
30 to < 40 Gy	703 ± 10	- 0.13 (±0.03)	0.0005
40 to < 50 Gy	699 ± 12	- 0.14 (±0.03)	< 0.0001
50 to < 54 Gy	705 ± 14	- 0.19 (±0.03)	< 0.0001
54 to 59 Gy	738 ± 25	- 0.17 (±0.03)	0.01

Table 3. Changes in white matter T1 as a function of radiation dose according to a random coefficient mixed model using all WM T1 data collected in the study. The p value shown tests for the significance of the change of T1 over time at each of the radiation doses listed. There was no significant change in T1 in white matter that received less than 20 Gy.

Gray matter T1 as a function of radiation dose

Radiation dose	Intercept (+SD)	Slope (+SD)	p-value
< 5 Gy	1095 \pm 17	- 0.09 (\pm 0.06)	NS
5 to < 10 Gy	1088 \pm 16	- 0.10 (\pm 0.06)	NS
10 to < 20 Gy	1090 \pm 16	- 0.10 (\pm 0.06)	NS
20 to < 30 Gy	1089 \pm 18	- 0.05 (\pm 0.07)	NS
30 to < 40 Gy	1067 \pm 23	- 0.03 (\pm 0.08)	NS
40 to < 50 Gy	1053 \pm 21	- 0.01 (\pm 0.06)	NS
50 to < 54 Gy	1014 \pm 24	- 0.00 (\pm 0.10)	NS
54 to 59 Gy	1008 \pm 20	- 0.15 (\pm 0.06)	NS

Table 4. Change in gray matter T1 as a function of radiation dose according to a random coefficient mixed model using all GM T1 data collected in the study. The p value shown tests for the significance in the change in T1 over time at each of the radiation doses listed. There was no significant change in T1 over time in any of the gray matter tissues.

White matter and gray matter T1 as a function of radiation dose category

Interval	< 20 Gy	≥ 20 Gy	p-value	< 50 Gy	≥ 50 Gy	p-value
Pre-RT	710	705	NS	1093	1059	0.0001
(± SD)	(± 13)	(± 13)		(± 20)	(± 21)	
Week 3	701	694	NS	1077	1052	0.008
(± SD)	(± 8)	(± 8)		(± 20)	(± 21)	
Week 5	713	704	NS	1103	1064	0.0001
(± SD)	(± 9)	(± 9)		(± 17)	(± 18)	
Week 13	709	705	NS	1067	1028	0.0001
(± SD)	(± 9)	(± 9)		(± 15)	(± 16)	
Week 26	708	689	0.001	1081	1057	0.002
(± SD)	(± 9)	(± 8D)		(± 19)	(± 19)	
Week 40	694	674	0.0009	1073	1037	0.0002
(± SD)	(± 13)	(± 13)		(± 17)	(± 18)	
Week 53	702	680	0.0007	1043	1020	0.04
(± SD)	(± 13)	(± 13)		(± 19)	(± 21)	

Table 5. Comparison of white matter T1 and gray matter T1 as a function of RT dose category at various times following treatment. P-value indicates where or not there was a significant difference between the T1 values in the WM that received less than 20 Gy versus the WM that received 20 Gy or greater and in the GM that received less than 50 Gy versus the GM that received 50 Gy or greater.

Baseline T1 values in white and gray matter according to tumor location

Patient group	Intercept (± SD)	P=	Age factor (± SD)	P=	Slope (± SD)	P=
Gray matter						
All patients	1032 (± 33)	0.0001	- 14.1 (± 3.1)	0.0001	- 0.8 (± 0.3)	0.03
IT tumors	1260 (± 36)	0.0001	- 13.5 (± 4.0)	0.002	- 2.2 (± 0.7)	0.002
ST tumors	1210 (± 51)	0.0001	- 13.5 (± 4.0)	0.002	- 0.4 (± 0.4)	NS
White matter						
All patients	765 (± 22)	0.0001	- 5.9 (± 2.0)	0.008	- 0.2 (± 0.2)	NS
IT tumors	795 (± 24)	0.0001	- 5.4 (± 2.5)	0.05	- 1.1 (± 0.3)	0.005
ST tumors	739 (± 33)	0.0001	- 5.4 (± 2.5)	0.05	0.1 (± 0.2)	NS

Table 6. The relationship between T1 in gray matter and white matter at baseline according to where the tumor is located. Since T1 was measured before radiation was given, the T1 pre-treatment is a function of tissue proximity to the tumor. This relationship is described by the equation: $T1 = [\text{intercept}] + [\text{age factor}] * \text{age (in years)} + [\text{slope}] * \text{radiation dose}$, where the values in brackets are from the table above.

REFERENCES:

1. Moss, W. "Historical Perspective of Normal Tissue Tolerance or Stumbling Along the Pathway of Dose Response to Necrosis and Back." Radiation Tolerance of Normal Tissue. Eds. J.M. Vaeth and J.L. Meyer. New York: Karger, 1988. 1-6.
2. Gottfried, K.D., and G. Penn, eds. Radiation in Medicine: A Need for Regulatory Reform. Washington, D.C.: National Academy Press, 1996.
3. Deeley, T. Principles of Radiation Therapy. Boston: Butterworths, 1976.
4. Shrieve DC, Alexander E, Black PM, *et al*. Treatment of patients with primary glioblastoma multiforme with standard postoperative radiotherapy and radiosurgical boost: prognostic factors and long-term outcome. *J Neurosurg* 1999; 90: 72-77.
5. DeAngelis LM. Brain Tumors. *N Engl J Med* 2001; 344: 114-123.
6. Schuleiss TE, Kun LE, Ang KK, *et al*. Radiation response of the central nervous system. *Int J Radiat Oncol Biol Phys* 1995; 31: 1093-1112.
7. Leibel SA, Ling CC, Kutcher GJ, *et al*. The biological basis for conformational three-dimensional radiation therapy. *Int J Radiat Oncol Biol Phys* 1991; 21: 805-811.
8. Raymond-Speden E, Tripp G, Lawrence B, *et al*. Intellectual, neuropsychological, and academic functioning in long-term survivors of leukemia. *J Pediatr Psychol* 2000; 25: 59-68.
9. Grill J, Renaux VK, Bulteau C, *et al*. Long-term intellectual outcome in children with posterior fossa tumors according to radiation doses, and volumes. *Int J Radiat Oncol Biol Phys* 1998; 45: 137-145.
10. Vigliani MC, Duyckaerts C, Hauw JJ, *et al*. Dementia following treatment of brain tumors with radiotherapy administered alone or in combination with nitrosourea-based chemotherapy: A clinical and pathological study. *J Neurooncol* 1999; 41: 137-149.
11. Kun L, Mulhern RK, Crisco JJ. Quality of life in children treated for brain tumors: intellectual, emotional, and academic function. *J Neurosurg* 1983; 58: 1-6.
12. Meadows A, Silberg J. Delayed consequences of therapy for childhood cancer. *Cancer* 1985; 35: 271-286.
13. Packer RJ, Sutton LN, Atkins TE, *et al*. A prospective study of cognitive function in children receiving whole-brain radiotherapy and chemotherapy: 2-year results. *J Neurosurg* 1989; 70: 707-713.
14. Carpentieri SC, Mulhern RK, Douglas S, *et al*. Behavioral resiliency among children surviving brain tumor: A longitudinal study. *J Clin Child Psychol* 1993; 22: 236-246.
15. Ris MD, Noll RB. Long-term neurobehavioral outcome in pediatric brain tumor patients: Review and methodological critique. *J Clin Exp Neuropsychol* 1994; 16: 21-42.
16. Mulhern RK, Reddick WE, Palmer SL, *et al*. Neurocognitive deficits in medulloblastoma survivors and white matter loss. *Ann Neurol* 1999; 46: 834-841.
17. Mulhern RK, Kepner JL, Thomas PR, *et al*. Neuropsychological functioning of survivors of childhood medulloblastoma randomized to receive conventional or reduced-dose CSI: A Pediatric Oncology Group study. *J Clin Oncol* 1998; 16: 1723-1728.
18. Curnes JT, Laster DW, Ball MR, *et al*. MRI of radiation injury to the brain. *Am J Roentgenol* 1986; 147: 119-124.

19. Curran WJ, Hecht-Leavitt C, Shut L, *et al.* Magnetic resonance imaging of cranial radiation lesions. *Int J Radiat Oncol Biol Phys* 1987; 13: 1093-1098.
20. Packer RJ, Zimmerman RA, Bilaniuk LT. Magnetic resonance imaging in the evaluation of treatment-related central nervous system damage. *Cancer* 1986; 58: 635-640.
21. Constine LS, Konski A, Ekholm S, *et al.* Adverse effects of brain irradiation correlated with MR and CT imaging. *Int J Radiat Oncol Biol Phys* 1988; 15: 319-330.
22. Kramer JH, Norman D, Brant-Zawadzki M, *et al.* Absence of white matter changes on magnetic resonance imaging in children treated with CNS prophylaxis therapy for leukemia. *Cancer* 1988; 61: 928-930.
23. Steen RG, Koury M, Granja CI, *et al.* Effect of ionizing radiation on the human brain: White matter and gray matter T1 in pediatric brain tumor patients treated with conformal radiation therapy. *J Radiat Oncol Biol Phys* 2001; 49: 79-91.
24. Steen RG, Gronemeyer SA, Kingsley PB, *et al.* Precise and accurate measurement of proton T1 in human brain in vivo: Validation and preliminary clinical application. *J Magn Reson Imag* 1994; 4: 681-691.
25. Cho S, Jones D, Reddick WE, *et al.* Establishing norms for age-related changes in proton T1 of human brain tissue in vivo. *Magn Reson Imaging* 1997; 15: 1133-1143.
26. Steen RG, Ogg R, Reddick WE, *et al.* Age-related changes in the pediatric brain: Quantitative magnetic resonance (qMRI) provides evidence of maturational changes during adolescence. *Am J Neuroradiol* 1997; 18: 819-828.
27. Steen RG, Reddick WE, Mulhern R, *et al.* Quantitative MRI of the brain in children with sickle cell disease reveals abnormalities unseen by conventional MRI. *J Magn Reson Imaging* 1998; 8: 535-543.
28. Steen RG, Xiong X, Mulhern RK, *et al.* Subtle brain abnormalities in children with sickle cell disease: Relationship to blood hematocrit. *Ann Neurol* 1999; 45: 279-286.
29. Steen RG, Reddick WE, Ogg RJ. More than meets the eye: Significant regional heterogeneity in human cortical T1. *Magn Reson Imaging* 2000; 18: 361-368.
30. Reddick WE, Ogg RJ, Steen RG, *et al.* Statistical error mapping for reliable quantitative T1 imaging. *J Magn Reson Imaging* 1996; 6: 244-249.
31. Kingsley PB, Ogg RJ, Reddick WE, *et al.* Correlation of errors caused by imperfect inversion pulses in MR imaging measurement of T1 relaxation times. *Magn Reson Imaging* 1997; 16: 1049-1055.
32. Reddick WE, Glass JO, Cook EN, *et al.* Automated segmentation and classification of multispectral magnetic resonance images of brain using artificial neural networks. *IEEE Trans Med Imaging* 1997; 16: 911-918.
33. Reddick WE, Mulhern RK, Elkin TD, *et al.* A hybrid neural network analysis of subtle brain volume differences in children surviving brain tumors. *Magn Reson Imaging* 1998; 16: 413-421.
34. Glass JO, Reddick WE, Yo V, *et al.* Hybrid artificial neural network segmentation of precise and accurate inversion recovery (PAIR) images from normal human brain. *Magn Reson Imaging* 2001; in press.
35. International Commission of Radiation Units and Measurements (ICRU). ICRU Report 50. Dose specification for reporting external beam therapy with photons and

- electrons. Washington, DC: International Commission and Radiation Units and Measurements; 1978 (ICRU report issued September 1993).
36. Rutter CM, Elashoff RM. Analysis of longitudinal data: Random coefficient regression modeling. *Stat Med* 1994; 13: 1211-1231.
 37. Little RC, Milliken GA, Stroup WS, *et al.* SAS System for mixed models. Cary, NC: SAS Institute; 1996.
 38. Fike JR, Cann CE, Turowski K, *et al.* Radiation dose response of normal brain. *Int J Radiat Oncol Biol Phys* 1988; 14: 63-70.
 39. Burger PC, Mahaley MS, Dudka L, *et al.* The morphologic effects of radiation administered therapeutically for intracranial gliomas: A postmortem study of 25 cases. *Cancer* 1979; 44: 1256-1272.
 40. Ball WS, Preneger EC, Ballard ET. Neurotoxicity of radio/chemotherapy in children: Pathologic and MR correlation. *Am J Neuroradiol* 1992; 13: 761-776.
 41. Asai A, Matsutani M, Kohno T, *et al.* Subacute brain atrophy after radiation therapy for malignant brain tumor. *Cancer* 1989; 63: 1962-1974.
 42. O'Conner MM, Mayberg MR. Effects of radiation on cerebral vasculature: A review. *Neurosurgery* 2000; 46: 138-151.
 43. Wenz F, Rempp K, Hess T, *et al.* Effect of radiation on blood volume in low-grade astrocytomas and normal brain tissue: quantification with dynamic susceptibility contrast MR imaging. *Am J Roentgenol* 1996; 166: 187-193.
 44. Chungani DC, Sundram BS, Behen M, *et al.* Evidence of altered energy metabolism in autistic children. *Prog Neuropsychopharmacol Biol Psychiatry* 1999; 23: 635-641.